Z. Phys. A – Atomic Nuclei 330, 63–68 (1988)

Zeitschrift für Physik A
Atomic Nuclei

β-Delayed Neutron Emission of ^{15}B, ^{18}C, ^{19,20}N, ^{34,35}Al and ^{39}P ⋆

A.C. Mueller[1], D. Bazin[1], W.D. Schmidt-Ott⋆⋆[1], R. Anne[1], D. Guerreau[1], D. Guillemaud-Mueller[1], M.G. Saint-Laurent[1], V. Borrel[2], J.C. Jacmart[2], F. Pougheon[2], and A. Richard[2]

[1] GANIL, Caen, France
[2] IPN, Orsay, France

Received January 4, 1988

The isotopes ^{15}B, ^{18}C, ^{19,20}N, ^{34,35}Al and ^{39}P have been produced as projectile-like fragments from the interaction of a ^{86}Kr beam of 45 MeV/u from GANIL with a ^{181}Ta target. Separated by the 0° magnetic analyser LISE, the nuclei are identified by means of a $\Delta E-E$ semiconductor telescope. It is surrounded, in a geometry close to 4π, by a thin plastic scintillator (NE 102) and a large volume liquid scintillator (NE 213) for the detection of betas and neutrons, respectively, from the decay of the implanted nuclei. By observation of the β-delayed neutrons, the half-lives $T_{1/2}$ and neutron emission probabilities P_n have been measured. The $T_{1/2}$ of ^{18}C, ^{20}N, ^{35}Al, ^{39}P and P_n of ^{18}C, ^{19,20}N, ^{34,35}Al and ^{39}P are determined for the first time. For the isotopes ^{17}C, ^{36,37}Si and ^{38}P upper limits of P_n are deduced.

PACS: 25.70.Np; 23.40.−s; 27.30.+t

I. Introduction

During the past years, a fruitful source for producing and studying light neutron-rich isotopes has become available: the fragmentation of Ar and Kr beams of intermediate energy from the GANIL cyclotrons has allowed, so far, the identification of new nuclei [1, 2, 3] as well as γ-spectroscopy [4] and direct mass measurements [5, 6] of hitherto unaccessible species. The increasing distance of these nuclei to the valley of β-stability translates into increasing values of Q_β, the energy available in their β-decay which eventually open up the window for decay into particle-unstable states of the daughter nuclei. The observation of the delayed neutrons from such a decay being coincident with the electrons provides a valuable experimental tool for measuring β-decay half-lives at very low counting rates. This has been shown for the most neutron-rich Na, Mg and K, Ca isotopes [7, 8] where a total coincidence detection efficiency of 30% was obtained by means of a liquid scintillator neutron counter. Since these experiments have been performed at an on-line isotope separator, they were limited to alcaline elements and their descendants. This is due to the chemical selectivity of the target/ionsource combination. Since this restriction is not present for a recoil-type separator, it was tempting to adapt a similar neutron counter to the spectrometer LISE [9].

It is the scope of the present paper to describe a first experiment which has been made with neutron-rich fragments, in the range from boron to phosphorus isotopes, obtained from a ^{86}Kr beam of 45 MeV/u incident energy onto a 83 mg/cm^2 ^{181}Ta target.

II. Experimental Set-Up and Procedure

The experimental set-up (see Fig. 1) mainly consists of four parts: *i)* the magnetic recoil-spectrometer LISE which separates the produced radioactive isotopes according to their mass-to-charge ratio A/Z. *ii)* a semiconductor detector telescope, at the exit of

⋆ Experiment performed at the French National Heavy-Ion Facility GANIL at Caen

⋆⋆ Permanent address: II. Physikalisches Institut, Universität Göttingen, D-3400 Göttingen, Federal Republic of Germany

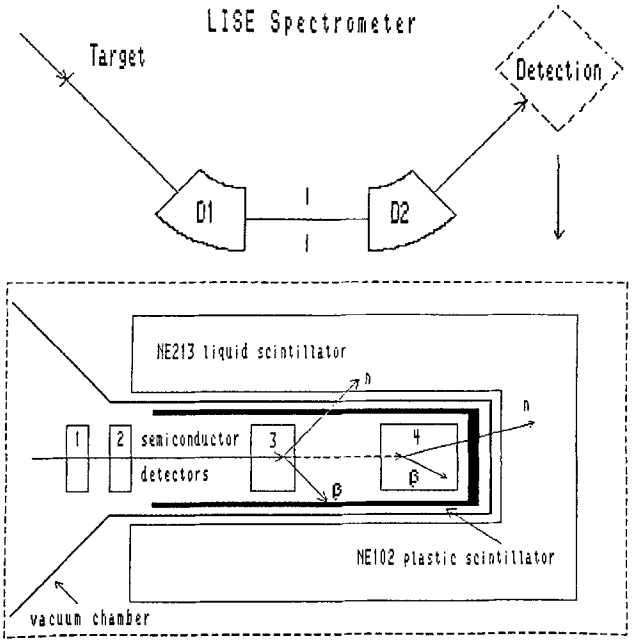

Fig. 1. Schematical experimental set-up. For details see text

LISE, in which the nuclei are implanted and which ensures their identification in A and Z by means of a measurement of their energy loss ΔE, total energy E and time-of-flight through LISE. *iii)* a detector for β-neutron coincidences, which surrounds the semiconductor telescope in a geometry which is close to 4π. *iv)* the data acquisition system and electronic overall control of the experiment. These parts are briefly presented in the following paragraphs.

II.1. LISE

The layout, principle and mode-of-operation of the magnetic spectrometer LISE have been described elsewhere [9]. Therefore, it may be sufficient to limit ourselves here to a recall of the main points which are of importance for the present experiment: projectile-fragmentation reactions are characterized by very small momentum transfer between projectile and target. Consequently, the projectile-like fragments are emitted around 0° with a velocity which is close to the incident one. Assuming complete electronic stripping of the reaction products, which is fulfilled around 50 MeV/u up to $Z \lesssim 20$, a dipole magnet, placed at 0° provides their analysis according to A/Z.

The basic feature of LISE is that a second, consecutive dipole counteracts the dispersion of the first one. This provides double achromatism, as well in angle as in position, at the exit of the spectrometer.

Thus, it is possible to collect all the fragments in a rather small spot and to install 4π-detectors of

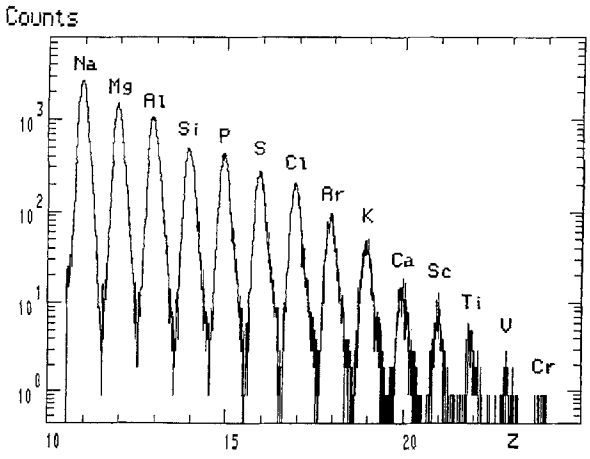

Fig. 2. Charge resolution for the 300 μ ΔE semiconductor detectors

a reasonable size for the decay studies. Furthermore, all trajectories between the production target and the collection point exhibit the same flight-path length of 18 m which is readily exploited for redundant particle identification.

The momentum acceptance of LISE is controlled, up to a maximum of $\Delta p/p = 5\%$, by variable aperture slits which are installed at the intermediate focal plane between the two dipoles. For the present experiment this momentum acceptance was limited to about 3%, corresponding to a value just inferior to the spacing between two adjacent ionic charge-states of the primary krypton beam. This is necessary in order to avoid pile-up effects in the semiconductor telescope and its associated electronics, due to the comparatively high counting rates of incompletely stripped krypton ions.

II.2. Semiconductor Telescope and Particle Identification

A four stage semiconductor telescope (See Fig. 1) was mounted inside a small vacuum chamber connected to the exit of LISE. It also houses the plastic-scintillator β-detector, whereas the neutron counter surrounding these detectors is mounted outside the vacuum chamber.

The first two semiconductor detectors, 1 and 2, are planar Si-junctions of 300 μ thickness and 450 mm^2 usable area. Since they exhibit excellent resolution, as can be seen in Fig. 2, a perfect (and redundant) charge identification of the passing heavy ions is assured. The total energy detectors, 3 and 4, have a thickness of 1 mm and 4 mm, respectively. This means, that fragments above ^{24}Mg will be stopped in detector 3 whereas the lighter ones will come to rest inside 4.

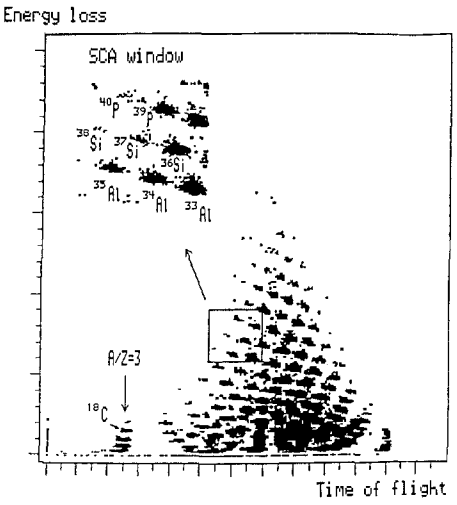

Fig. 3. Identification of the produced fragments in the matrix ΔE versus time-of-flight. Insert shows the selection of a given region of isotopes by single channel analysers for the half-life measurements (see Sect. II.4.)

The detectors are connected to charge and voltage sensitive preamplifiers in order to derive the ΔE, E and timing signals. Using the timing signal as "START" and a signal derived from the radiofrequency of the GANIL-accelerator as "STOP" of a time-to-amplitude converter, the time-of-flight through the spectrometer is acquired. This is due to the constant relationship of the cyclotron frequency phase and the time of impact of the beam pulses on the target. This frequency being typically 10 MHz, the start and stop signals are reversed in order to prevent unnecessary triggering. Thus, the isotopes with a higher value of A/Z are found to be on the lower end of the time-of-flight scale in Fig. 3. This figure, representing the bidimensional plot of ΔE versus time-of-flight, shows the straightforward isotope identification obtained this way. It also illustrates the characteristic separation in A/Z of the spectrometer since lines of constant time-of-flight, i.e. constant velocity, correspond to the isotopes of the same ratio A/Z.

II.3. The β-Neutron Detector

The principal β-detector consists of a tumbler-shaped NE102A plastic scintillator of 3 mm thickness, 200 mm length and 94 mm opening so as to house the collecting detectors 3 and 4 (see Fig. 1) and to allow to their electrical connections to be fed out. The scintillator is connected to a light guide which goes out of the vacuum chamber to a photomultiplier, cooled for reducing the noise from its photocathode.

The threshold for electron detection corresponded to about 200 keV. Since the energy loss for electrons in silicon, roughly 300 keV/mm, allows for a sufficiently high signal in the 4 mm semiconductor detector, the latter is also monitored for a β-decay signal after the implantation of a heavy ion.

For the neutron detector, a fast liquid scintillator, NE 213, has been chosen due to its $n-\gamma$ separation properties and for its insensitivity to thermal neutrons. Under the present experimental conditions, that is of special importance: a strong background of fast neutrons is generated by the impact of the primary heavy ion beam on the production target as well as the beam dump.

Despite of a heavy concrete shielding some neutrons are leaking, by consecutive reflection, through the chicanery between the production and the collection room of the LISE spectrometer. A thermalization constant of about 10 ms is observed for these neutrons which is due to the overall geometry of the installation.

In a "classical" neutron counter operating through degradation and capture of thermal neutrons, this would give rise to a time-dependent background. Considering the low counting rates for isotopes far off stability and that the expected half-lives are comparable to the time-dependence of the background, a serious experimental problem may result. The choice of the liquid scintillator NE 213, which detects neutrons via scattered recoiling protons proved to be insensitive to these problems.

Furthermore, the liquid scintillator NE 213 exhibits a pronounced $n-\gamma$ discrimination effect [10]. This is of interest to suppress γ-rays of activities which may be co-implanted or coming from a daughter activity. A cylindrical shielding of 1 cm of lead around the outside of the vacuum chamber further suppressed γ-background.

The vessel containing the liquid scintillator is built around this lead shield. Since neutrons following the decay of the implanted samples have to go across at least 9 cm of liquid, a good detection efficiency is achieved. For mechanical reasons, the vessel is composed of 3 independent parts which contain a total of 30 l of the scintillator NE 213. Five windows provide the connection to 5 inch diameter photomultipliers. The electronics for the $n-\gamma$ separation is designed according to suggestions made in [11].

Figure 4 shows the obtained $n-\gamma$ separation. The calibration with a $Am-Be$ source of known activity placed in the middle of the neutron counter gave a total detection efficiency of 55% for a threshold of 50 keV equivalent electron energy. This corresponds to a neutron detection threshold of about 400 keV [12].

In order to further reduce any residual background, the neutron counter was lodged inside a

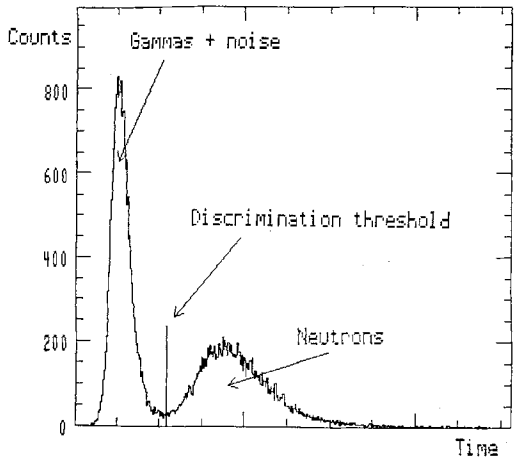

Fig. 4. $n-\gamma$ separation of the NE 213 neutron detector

housing made of 1 m thick concrete covered at its inside with 1 mm of cadmium.

According to the width of the signals coming from the β-detector and the 5 neutron-counters, a coincidence window of 250 ns was set.

II.4. Data Acquisition and Overall Control of the Experiment

The data acquisition consists of two independent systems connected together to a main computer by means of a microprocessor.

Thus, events of the first acquisition, responsible for the particle identification (energy and time-of-flight from the semiconductor detectors) and of the second acquisition (β-neutron counter) are chronologically stored onto the same magnetic tape. Each event is labelled by its time of arrival which is read from a quartz clock.

The experiment is controlled in the following way: In the normal condition the particle identification system is active, whereas the data taking of the β-neutron counter is disabled. Two single channel analysers define a window in the bidimensional matrix of ΔE vs. time-of-flight (see Fig. 3 and Sect. II.2). As soon as a particle is detected inside this window, a variable gate, adjustable in length to the expected decay time, is set. During this period, the cyclotron beam is switched off in order to prevent any further production and implantation of radioactive nuclei, and the second data acquisition is enabled. The combination of the information of the two data acquisitions by means of the microprocessor allows the on-line generation of the decay spectra. This technique is rather elegant because it correlates the observation of β-delayed neutrons to the information *that and which* nucleus was implanted, and therefore allows the simultaneous study of several emitters.

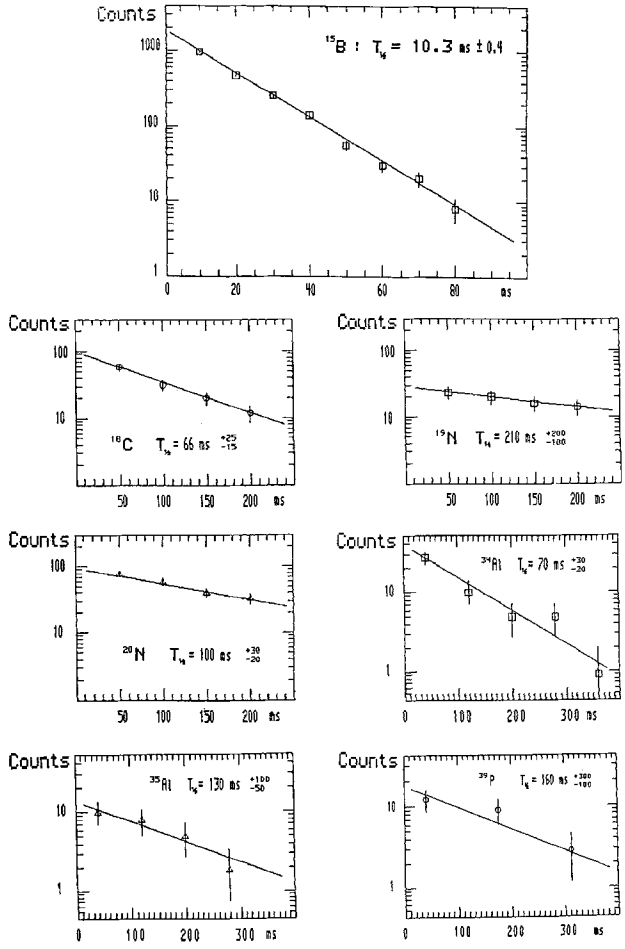

Fig. 5. β-decay for the isotopes ^{15}B, ^{18}C, ^{19,20}N, ^{34,35}Al and ^{39}P. The experimental data points are represented with their statistical error bars and the solid lines correspond to the fitting procedure explained in the text

III. Results and Discussion

The experiment has been made with two settings of the magnetic rigidity of the LISE spectrometer, 2.46 Tm and 2.28 Tm. With a thickness of 83 mg/cm^2 of the ^{181}Ta production target, this corresponds to nuclei around carbon and $A/Z=3$ and around aluminium and $A/Z=2.6$, respectively.

In principle, the off-line analysis was based on the on-line one. Additionally, special care was devoted to the selection of the neutron-γ discrimination threshold and the width of the β-neutron coincidence window. Figure 5 shows the decay curves of the β-delayed neutrons from ^{15}B, ^{18}C, ^{19,20}N, ^{34,35}Al and ^{39}P which are obtained this way. The solid lines through the experimental data points represent a fit performed in the following way: A χ^2-test was applied to a one-component decay with a constant background. This was justified since the minimum chi-square $\chi^2_{\min}$, calculated by varying the free parameter

Table 1. Experimental and theoretical β-half-lives

A_Z	$T_{1/2}$ (ms) experimental values		$T_{1/2}$ (ms) theoretical predictions			
	this work	other work	[a]	[b]	[c]	[d]
^{15}B	$10.4^{+0.3}_{-0.3}$	11 ± 1[e]; 8.8 ± 0.6[f]; 11 ± 2.8[g]	28.8	52	24	–
^{18}C	66^{+25}_{-15}	–	130	136	64	124
^{19}N	210^{+200}_{-100}	320 ± 100[h]; 205 ± 62[g]	184	171	287	590
^{20}N	100^{+30}_{-20}	–	66.5	94	100	439
^{34}Al	70^{+30}_{-20}	54 ± 12[h]	149	236	172	76
^{35}Al	130^{+100}_{-50}	–	161	251	125	33
^{39}P	160^{+300}_{-100}	–	448	504	890	93

[a, b] Gross theory by Takahashi [18] with Lorentzian-shaped (a) and Gaussian-shaped (b) Gamov-Teller resonance
[c] Gross theory improved by Tachibana et al. [17]; [d] Microscopic model by Klapdor et al. [20]. Other experimental results: [e] [14]; [f] [15]; [g] [16]; [h] [4]

half-life, number of emitting nuclei and background, was found to be around $\chi^2_{min} \simeq 1$ when allowing only for statistical error of the observed count rates. These calculations were made with the help of the FORTRAN code MINUIT [13]. In MINUIT, the one-standard-deviation error of a free parameter may be obtained through a deviation from its optimum value combined with a refitting of the other parameters until $\chi^2 = \chi^2_{min} + 1$ is reached. This often leads, especially at low statistics, to much larger and frequently also asymmetric error bars than the more generally used assumption of a parabolic behaviour of χ^2 around its minimum value. In our case, we have adopted this technique for the determination of the error of the half-life $T_{1/2}$ and the neutron emission probability P_n. The latter has been obtained by calibrating the coincidence efficiency of the detector with the known value of $P_n = 100\%$ [14] for the isotope ^{15}B. An efficiency of 21% was found from the comparison of the precisely known number of the implanted ^{15}B nuclei to the number of detected β-delayed neutrons from its decay. It should be noted, however, that, because of the threshold settings for the β- and neutron-detection a similar spectrum shape as the one in ^{15}B is presupposed for all investigated isotopes.

The present experimental results of β-half-lives are listed in Table 1 and those for the neutron emission probability in Table 2. The decay of ^{18}C, ^{20}N, ^{35}Al and ^{39}P are reported for the first time. One should

Table 2. Experimental and theoretical neutron emission probabilities

A_z	P_n (%) experimental	P_n (%) theoretical predictions		
	this work	[a]	[b]	[c]
^{15}B	(100)[d]	30	75	75
^{17}C	<11	5.6	15	20
^{18}C	25 ± 4.5	21	51	22
^{19}N	33^{+34}_{-11}	12	29	37
^{20}N	53^{+11}_{-7}	30	77	32
^{34}Al	54 ± 12	9.2	35	20
^{35}Al	87^{+37}_{-25}	26.5	63	44
^{36}Si	<10	3.9	11	6.5
^{37}Si	<15	6.1	20	10
^{38}P	<10	1.4	4.5	7.2
^{39}P	41^{+32}_{-16}	12.4	30	22

[a] Gross theory [18] with Lorentzian-shaped Gamov-Teller resonance
[b] Gross theory [18] with Gaussian-shaped Gamov-Teller resonance
[c] Fitting procedure by Kratz and Hermann [21]
[d] Experimental result from [14]

note, despite of the almost perfect fit of Fig. 5 for one-standard-deviation error, that the statistics is low in some cases. Performing the error analysis with a 95% confidence level (i.e. two-standard-deviation error) yields, for ^{35}Al and ^{39}P, compatibility with the non-observation of any decay. Agreement between present values and earlier reported half-lives is observed for ^{19}N and ^{34}Al. Our result for ^{15}B is in accordance with [14] and somewhat larger than another reported value [15], however, a reevaluation of the latter data [16] yielded a result being in the lines with the present one.

The comparison with available theoretical half-life predictions gives satisfactory accordance with the improved gross theory of β-decay which recently has been proposed by Tachibana et al. [17]. In this table, the predictions of the "old" gross theory obtained by injecting into the code of Takahashi et al. [18] the values of the mass table by Wapstra et al. [19] and of the microscopic model [20] are given as well. For the present region of isotopes the gross theory is giving a better overall description.

Since the present P_n values represent the first experimental results for a number of light isotopes, they are essayed for a comparison with calculated neutron emission probabilities. Table 2 shows the result of the calculation of the P_n values by means of the gross

theory [18] for two different β-strength distributions. Also the fitting procedure [21], derived from experimental data mainly in the fission product region was applied to the present region of light isotopes with the help of the Wapstra mass table [19]. A reasonable agreement is observed in all instances with a slight preference of the latter calculated values.

IV. Summary and Prospects

In this experiment, we were able to produce a series of nuclei situated at the present border-line of the known isotopes.

The technique of correlating the identification of the produced fragments to the detection of the coincidence between betas and neutrons allowed a measurement of the β-half-lives $T_{1/2}$ and the delayed neutron emission probabilities P_n.

As is discussed elsewhere [22], however, the presently used production with ^{86}Kr projectiles of an energy of 45 MeV/u is still influenced by energy-dissipative processes leading to fragment excitation which in turn reduces strongly the production of very neutron-rich nuclei because of particle evaporation.

An extension of the present experiment is envisaged in various ways. First of all to take advantage for isotope production of ^{48}Ca projectiles which are expected to induce a reaction being more closer to high-energy fragmentation already at GANIL energies [23]. Furthermore, to use the fragmentation of heavier projectiles for production of heavy neutron-rich isotopes as soon as relativistic energies are available. This program being of special interest in respect to astrophysics in order to trace the *r*-process synthesis of medium-mass and of heavy elements.

The technical assistance of F. Geoffroy, R. Hue, Y. Huguet and A. Latimier during the preparation was of decisive influence for the success of this experiment.

References

1. Langevin, M., Quiniou, E., Bernas, M., Galin, J., Jacmart, J.C., Pougheon, F., Anne, R., Détraz, C., Guerreau, D., Guillemaud-Mueller, D., Mueller, A.C.: Phys. Lett. **150** B, 71 (1985)
2. Guillemaud-Mueller, D., Mueller, A.C., Guerreau, D., Pougheon, F., Anne, R., Bernas, M., Galin, J., Jacmart, J.C., Langevin, M., Naulin, F., Quiniou, E., Détraz, C.: Z. Phys. A – Atoms and Nuclei **322**, 415 (1985)
3. Pougheon, F., Guillemaud-Mueller, D., Quiniou, E., Saint-Laurent, M.G., Anne, R., Bazin, D., Bernas, M., Guerreau, D., Jacmart, J.C., Hoath, S.D., Mueller, A.C., Détraz, C.: Europhys. Lett. **2** (7), 505 (1986)
4. Dufour, J.P., Del Moral, R., Fleury, A., Hubert, F., Jean, D., Pravikoff, M.S., Delagrange, H., Geissel, H., Schmidt, K.H.: Z. Phys. A – Atomic Nuclei **324**, 487 (1986)
5. Gillibert, A., Bianchi, L., Cunsolo, A., Fernandez, B., Foti, A., Gastebois, J., Gregoire, Ch., Mittig, W., Peghaire, A., Schutz, Y., Stephan, C.: Phys. Lett. B **176**, 317 (1986)
6. Gillibert, A., Mittig, W., Bianchi, L., Cunsolo, A., Fernandez, B., Foti, A., Gastebois, J., Gregoire, Ch., Schutz, Y., Stephan, C.: Phys. Lett. B **192**, 39 (1987)
7. Langevin, M., Détraz, C., Guillemaud-Mueller, D., Mueller, A.C., Thibault, C., Touchard, F., Klotz, G., Miehé, C., Walter, G., Epherre, M., Richard-Serre, C.: Phys. Lett. B **130**, 251 (1983)
8. Langevin, M., Détraz, C., Guillemaud-Mueller, D., Mueller, A.C., Thibault, C., Touchard, F., Epherre, M.: Nucl. Phys. A **414**, 152 (1984)
9. Anne, R., Bazin, D., Mueller, A.C., Jacmart, J.C., Langevin, M.: Nucl. Instrum. Methods A **257**, 215 (1987)
10. Winyard, R.A., Lutkin, J.E., McBeth, G.W.: Nucl. Instrum. Methods **95**, 141 (1971)
11. Randers-Pehrson, G., Finlay, R.W., Carter, D.E.: Nucl. Instrum. Methods **215**, 433 (1983)
12. Cecil, R.A., Anderson, B.D., Madey, R.: Nucl. Instrum. Methods **161**, 439 (1979)
13. James, F., Roos, M.: Comp. Phys. Comm. **10**, 343 (1975)
14. Dufour, J.P., Beraud-Sudreau, S., Del Moral, R., Emmermann, H., Fleury, A., Hubert, F., Poirot, C., Pravikoff, M.S., Frehaut, J., Beau, M., Bertin, A., Giraudet, G., Huck, A., Klotz, G., Miehé, C., Richard-Serre, C., Delagrange, H.: Z. Phys. A – Atoms and Nuclei **319**, 237 (1984)
15. Curtin, M.S., Harwood, L.H., Nolen, J.A., Sherill, B., Xie, Z.Q., Brown, B.A.: Phys. Rev. Lett. **56**, 34 (1986)
16. Samuel, M., Brown, B.A., Mikolas, D., Nolen, J.A., Sherill, B., Stevenson, J., Winfield, J., Xie, Z.Q.: Annual Report of the Cyclotron Laboratory, Michigan State University, May 1987, p. 60, East Lansing, Michigan
17. Tachibana, T., Ohsugi, S., Yamada, M.: Proceedings of the 5th International Conference on Nuclei far from Stability, September 14–19, 1987, Rosseau Lake, Ontario, Canada. In: AIP Conference Proceedings. Towner I.S. (ed.), p. 614. New York 1988
18. Takahashi, K.: Prog. Theo. Phys. **47**, 1500 (1972)
19. Wapstra, A.H., Audi, G.: Nucl. Phys. A **432**, 1 (1985)
20. Klapdor, H.V., Metzinger, J., Oda, T.: At. Data Nucl. Data Tables **31**, 81 (1984)
21. Kratz, K.L., Herman, G.: Z. Phys. A – Atoms and Nuclei **263**, 435 (1973)
22. Bazin, D., Anne, R., Guerreau, D., Guillemaud-Mueller, D., Mueller, A.C., Saint-Laurent, M.G., Schmidt-Ott, W.D., Borrel, V., Jacmart, J.C., Pougheon, F., Richard, A.: Proceedings of the 5th International Conference on Nuclei far from Stability, September 14–19, 1987, Rosseau Lake, Ontario, Canada. In: AIP Conference Proceedings. Towner I.S. (ed.), p. 722. New York 1988
23. Guerreau, D.: J. Phys. (Paris) C **4–8**, 205 (1986)

A.C. Mueller, D. Bazin, R. Anne, D. Guerreau,
D. Guillemaud-Mueller, M.G. Saint-Laurent
GANIL
BP 5027
F-14021 Caen Cedex
France

W.D. Schmidt-Ott
II. Physikalisches Institut
Universität Göttingen
Bunsenstrasse 7–9
D-3400 Göttingen
Federal Republic of Germany

V. Borrel, J.C. Jacmart, F. Pougheon, A. Richard
IPN
BP 1
F-91406 Orsay Cedex
France